Developmental Biology ■ (■■■■) ■■■–■■■

Contents lists available at ScienceDirect

Developmental Biology

journal homepage: www.elsevier.com/locate/developmentalbiology

The hyaloid vasculature facilitates basement membrane breakdown during choroid fissure closure in the zebrafish eye

Andrea James [a,b,1], Chanjae Lee [a,1], Andre M. Williams [a], Krista Angileri [a,b], Kira L. Lathrop [b,d], Jeffrey M. Gross [a,b,c,*]

[a] Department of Molecular Biosciences, Institute for Cellular and Molecular Biology, The University of Texas at Austin, Austin, TX 78712, United States
[b] Department of Ophthalmology, Louis J. Fox Center for Vision Restoration, The University of Pittsburgh School of Medicine, Pittsburgh, PA 15213, United States
[c] Department of Developmental Biology, The University of Pittsburgh School of Medicine, Pittsburgh, PA 15213, United States
[d] Department of Bioengineering, University of Pittsburgh Swanson School of Engineering, Pittsburgh, PA 15213, United States

ARTICLE INFO

Article history:
Received 5 April 2016
Received in revised form
9 September 2016
Accepted 9 September 2016

ABSTRACT

A critical aspect of vertebrate eye development is closure of the choroid fissure (CF). Defects in CF closure result in colobomas, which are a significant cause of childhood blindness worldwide. Despite the growing number of mutated loci associated with colobomas, we have a limited understanding of the cell biological underpinnings of CF closure. Here, we utilize the zebrafish embryo to identify key phases of CF closure and regulators of the process. Utilizing Laminin-111 as a marker for the basement membrane (BM) lining the CF, we determine the spatial and temporal patterns of BM breakdown in the CF, a prerequisite for CF closure. Similarly, utilizing a combination of *in vivo* time-lapse imaging, β-catenin immunohistochemistry and F-actin staining, we determine that tissue fusion, which serves to close the fissure, follows BM breakdown closely. Periocular mesenchyme (POM)-derived endothelial cells, which migrate through the CF to give rise to the hyaloid vasculature, possess distinct actin foci that correlate with regions of BM breakdown. Disruption of *talin1*, which encodes a regulator of the actin cytoskeleton, results in colobomas and these correlate with structural defects in the hyaloid vasculature and defects in BM breakdown. *cloche* mutants, which entirely lack a hyaloid vasculature, also possess defects in BM breakdown in the CF. Taken together, these data support a model in which the hyaloid vasculature and/or the POM-derived endothelial cells that give rise to the hyaloid vasculature contribute to BM breakdown during CF closure.

1. Introduction

In all vertebrates, eye development begins with the evagination of optic primordia from the diencephalon. The optic primordia subsequently adopt vesicle-like structures, and as the lateral edges of the vesicles begin to fuse, each invaginates to form a bilayered cup. The outer layer of the cup gives rise to the retinal pigment epithelium (RPE) and the inner layer gives rise to the retina. Fusion between the prospective RPE and retina occurs at the choroid fissure (CF), a distinct region of the ventral optic cup. Prior to fusion, the hyaloid vasculature enters the eye through the CF and the retinal ganglion cell axons exit through it. Once these developmental events have occurred, CF closure (CFC) is critical for containment of the retina and RPE within the optic cup. Defects in ventral optic cup formation or CFC result in colobomas (Graw, 2003; Gregory-Evans et al., 2004; Fitzpatrick and van Heyningen, 2005; Chang et al., 2006). The incidence of colobomas ranges from 2.6 in 10,000 births in the U.S. to 7.5 in 10,000 births in China, and colobomas are estimated to be present in 3–11% of all blind children worldwide (Onwochei et al., 2000). Colobomas are also present in over 50 human genetic disorders (OMIM), often associated with other ocular abnormalities like microphthalmia (Bermejo and Martinez-Frias, 1998).

Despite a significant amount of genetic research to identify coloboma loci, causative mutations have been identified in less than 20% of coloboma patients (Gregory-Evans et al., 2004; Fitzpatrick and van Heyningen, 2005; Chang et al., 2006). Moreover, we lack a comprehensive mechanistic understanding of the cellular and molecular regulation of CF closure in the human eye or in any of the animal model systems utilized for modeling human eye development and disease. Studies from a number of laboratories, and from both human genetics and experimental analyses in a

* Corresponding author at: Department of Ophthalmology, Louis J. Fox Center for Vision Restoration, The University of Pittsburgh School of Medicine, Pittsburgh, PA 15213, United States.
E-mail address: grossjm@pitt.edu (J.M. Gross).
[1] These authors contributed equally to this work.

http://dx.doi.org/10.1016/j.ydbio.2016.09.008
0012-1606/

variety of animal systems, have identified a suite of gene products required for CFC (reviewed in Bibliowicz et al. (2011), Morris (2011) and Gestri et al. (2012)). These include: Pax2 (Sanyanusin et al., 1995; Torres et al., 1996; Macdonald et al., 1997; Bower et al., 2012), GDF3 and GDF6 (Asai-Coakwell et al., 2007; Ye et al., 2010), CHD7 (Bosman et al., 2005; Lalani et al., 2006; Bajpai et al., 2010), SALL2 (Kelberman et al., 2014), YAP1 (Williamson et al., 2014), VSX2 (Bar-Yosef et al., 2004), SMOC1 (Rainger et al., 2011), Sox11 (Pillai-Kastoori et al., 2014), Jnk1/2 (Weston et al., 2003), MAB21L2 (Rainger et al., 2014; Deml et al., 2015), and Vax1 and Vax2 (Barbieri et al., 2002; Take-uchi et al., 2003), as well as components of the Hedgehog (Schimmenti et al., 2003; Koudijs et al., 2008; Lee et al., 2008), Fibroblast growth factor (FGF) (Cai et al., 2013; Chen et al., 2013a; Atkinson-Leadbeater et al., 2014), Wnt (Liu et al., 2016), and Retinoic acid (RA) (Matt et al., 2008; See and Clagett-Dame, 2009; Lupo et al., 2011) signaling pathways. While the mechanisms underlying their requirements during CFC have not been fully elucidated in each case, many of these gene products act early in eye development to modulate key events in retinal growth and cell survival, optic cup morphogenesis and patterning that are ultimately required for CFC. Defects in any of these processes result in colobomas; however, these are likely an indirect consequence of defects in ventral optic cup formation or patterning, and not a direct function of the mutated gene product during CFC.

Indeed, we have a far more limited understanding of the later events in eye development that function to close the CF. Results from several studies link an inability to degrade the basement membrane (BM)/basal lamina that lines the CF to defects in CFC and colobomas. For example, deficiencies in RA signaling during the later stages of eye development in rats result in a retention of the BM lining the CF and colobomas (See and Clagett-Dame, 2009). Knockout or mutations in *Pax2/pax2* (Torres et al., 1996; Macdonald et al., 1997) or *Vax2* (Barbieri et al., 2002) also result in retention of the CF BM and colobomas. Much like BM breakdown, the mechanism of tissue fusion that ultimately seals the tightly apposed sides of the CF during CFC is also poorly understood. Roles for adhesion regulators like N-cadherin (Erdmann et al., 2003; Masai et al., 2003) and α-catenin (Chen et al., 2012) have been identified in mediating CFC, but the morphogenetic events leading to tissue fusion in the CF and their cellular underpinnings have not been elucidated in any system.

To begin to identify the cellular and molecular underpinnings of these later aspects of CFC, we utilized the zebrafish embryo and a combination of fixed-sample and *in vivo* imaging in wild-type (WT) and mutant lines. We determined the spatial and temporal aspects of BM breakdown and tissue fusion during CFC, identifying unique characteristics of CF cells throughout the closure process. We identify BM membrane breakdown defects in the CF of *talin1* and *cloche* mutants, and these defects correlate with malformations in, or absence of, the periocular mesenchyme (POM)-derived hyaloid vasculature. Taken together, these data support a model in which the hyaloid vasculature itself, or the POM-derived endothelial cells that generate the hyaloid vasculature, facilitate BM breakdown during CFC.

2. Materials and methods

2.1. Animals

Zebrafish were maintained as described (Westerfield, 1995). Embryos were obtained and staged as described (Kimmel et al., 1995). We utilized the transgenic lines Tg(*fli1a:*eGFP) (Lawson and Weinstein, 2002), Tg(*sox10:*eGFP) (Wada et al., 2005), Tg(*sox10:*mRFP*)* (Kirby et al., 2006), Tg(*kdrl*:mCherry) and Tg(*kdrl*:moesin-GFP) (Wang et al., 2010). *tln1*$^{hi3093Tg/+}$ embryos (Amsterdam et al., 2004) were obtained from ZIRC (Eugene, OR, USA) and crossed with Tg(*kdrl*:mCherry). *tln1*^{hi3093tg} mutants were genotyped using these primers: 5′-ccaaacctacaggtggggtc-3′ and 5′-taccagcatttactcaacaggaac-3′. *cloche*^{m378} embryos (Stainier et al., 1995) were a kind gift of Dr. Beth Roman (University of Pittsburgh) and mutants were identified based on lack of blood flow at 48 hpf. All protocols used within this study were approved by the Institutional Animal Care and Use Committee of The University of Texas at Austin and The University of Pittsburgh School of Medicine, and conform to the National Institutes of Health Guide for the Care and Use of Laboratory Animals.

2.2. Microinjection of mRNAs

Capped mRNAs were synthesized with a mMESSAGE mMACHINE Sp6 kit (Life Technologies) and were injected into one-cell-stage embryos with the following amounts: 150 pg of *membrane-GFP* or 100 pg of *utrophin-GFP* (Burkel et al., 2007).

2.3. In situ hybridization

In situ hybridizations were performed as described (Jowett and Lettice, 1994). A *talin1 in situ* probe was synthesized from a partial cDNA cloned by RT-PCR with the following primers: 5′-tagcagtggcacagtcccgtattg-3′ and 5′-ttttttcttcctccaggcttg-3′. Embryos were subsequently cryosectioned and imaged, or immunostained in the case of *fli1a*:GFP and imaged.

2.4. Immunohistochemistry

Immunohistochemistry was performed as described (Uribe and Gross, 2007). Briefly, zebrafish embryos were fixed overnight in 4% paraformaldehyde, or 30 min at room temperature (for β-catenin), and then cryosectioned. Primary antibodies were used at the following dilutions: rabbit polyclonal anti-laminin (Sigma, #L9393), 1:200; mouse monoclonal anti-β-catenin (BD Biosciences, 610153), 1:250; and rabbit polyclonal anti-GFP (Life Technologies, A11122), 1:50. Phalloidin (Alexa Fluor 488 or 633, Invitrogen), DAPI or Sytox-Green were applied along with, or just prior to, the application of Cy2, Cy3 or Cy5 conjugated Goat anti-mouse or anti-rabbit IgG secondary antibodies (Jackson Labs).

2.5. Imaging

For sectioned embryos, imaging was performed with a Zeiss LSM5 Pascal or Olympus FV1200 confocal microscope. *In situ* cryosections were imaged utilizing a Leica DM2500 with a 100X oil immersion objective (Numerical aperture: 1.25). Brightfield images were captured on a Leica MZ16F stereomicroscope mounted with a DFC480 digital camera. *In vivo* time-lapse imaging was performed on a Leica TCS SP5 II confocal microscope equipped with a 25X (Numerical aperture: 0.95) water immersion objective as previously described (Hartsock et al., 2014), or an Olympus FV1200 with a 20X (Numerical aperture: 1.0) water immersion objective.

2.6. TUNEL staining

Embryos were fixed in 4% paraformaldehyde and cryosectioned. The sectioned tissues were permeabilized with 0.1% TritonX-100 in 0.1% sodium citrate and then treated with the TUNEL reaction mixture (Roche). Images were captured with a Zeiss LSM5 Pascal.

Please cite this article as: James, A., et al., (2016), http://dx.doi.org/10.1016/j.ydbio.2016.09.008

3. Results

3.1. Temporal and spatial dynamics of basement membrane breakdown during CF closure

To identify the cellular and molecular underpinnings of CFC in zebrafish, we first performed a detailed analysis of the temporal and spatial dynamics of CFC. In mouse and hamster, BM breakdown correlates with CFC (Geeraets, 1976; Hero, 1989, 1990). Laminin-111 (Lam-111) immunostaining was used as a marker for the BM lining the CF to determine whether this is also the case in zebrafish. Embryos were sectioned sagittally, at varying depths along the proximal-distal axis of the eye (Fig. 1A,N), and the presence or absence of Lam-111 assessed. We designated the vitreous cavity as "central" along the proximal-distal axis of the CF, as this was a fiducial marker easily identifiable in the continually growing eye over time. For Lam-111 immunohistochemistry, we then examined sections taken at 12 μm intervals proximal and distal of this central point.

Previous histological data suggested that CFC starts at 36 hpf (hour post fertilization) in zebrafish (Schmitt and Dowling, 1994), so we examined 36 hpf embryos in our initial assays (Fig. 1J-M). When Lam-111 distribution was examined in these eyes however, the BM was already absent/degraded in the central/proximal region of the CF (Fig. 1L), and was present or partially degraded in more distal regions (Fig. 1J,K). Examination of eyes from younger embryos (31 hpf) revealed that, despite the tight apposition of the sides of the CF, the BM remained intact at all proximal-distal depths (Fig. 1B-E; inset in Fig. 1D). By 34 hpf, BM breakdown had initiated and the BM separating the closely apposed sides of the CF was discontinuous (Fig. 1F-I, inset in Fig. 1H). Spatially, BM breakdown began in the central/proximal CF (Fig. 1F-I), and proceeded bi-directionally from this point (Fig. 1 J-M). Laminin-111 staining was mostly absent in the CF by 48 hpf (Fig. 1N-P) except in the most distal region of the eye in some embryos, where it was no longer detected at 60 hpf (*data not shown*).

TEM studies in mouse (Hero, 1989, 1990; Hero et al., 1991) and hamster (Geeraets, 1976) have also reported a correlation between cell death in the CF and CFC, although the functional relevance of this is unknown. TUNEL staining during zebrafish CFC did not identify any apoptotic cells in the CF (*data not shown*).

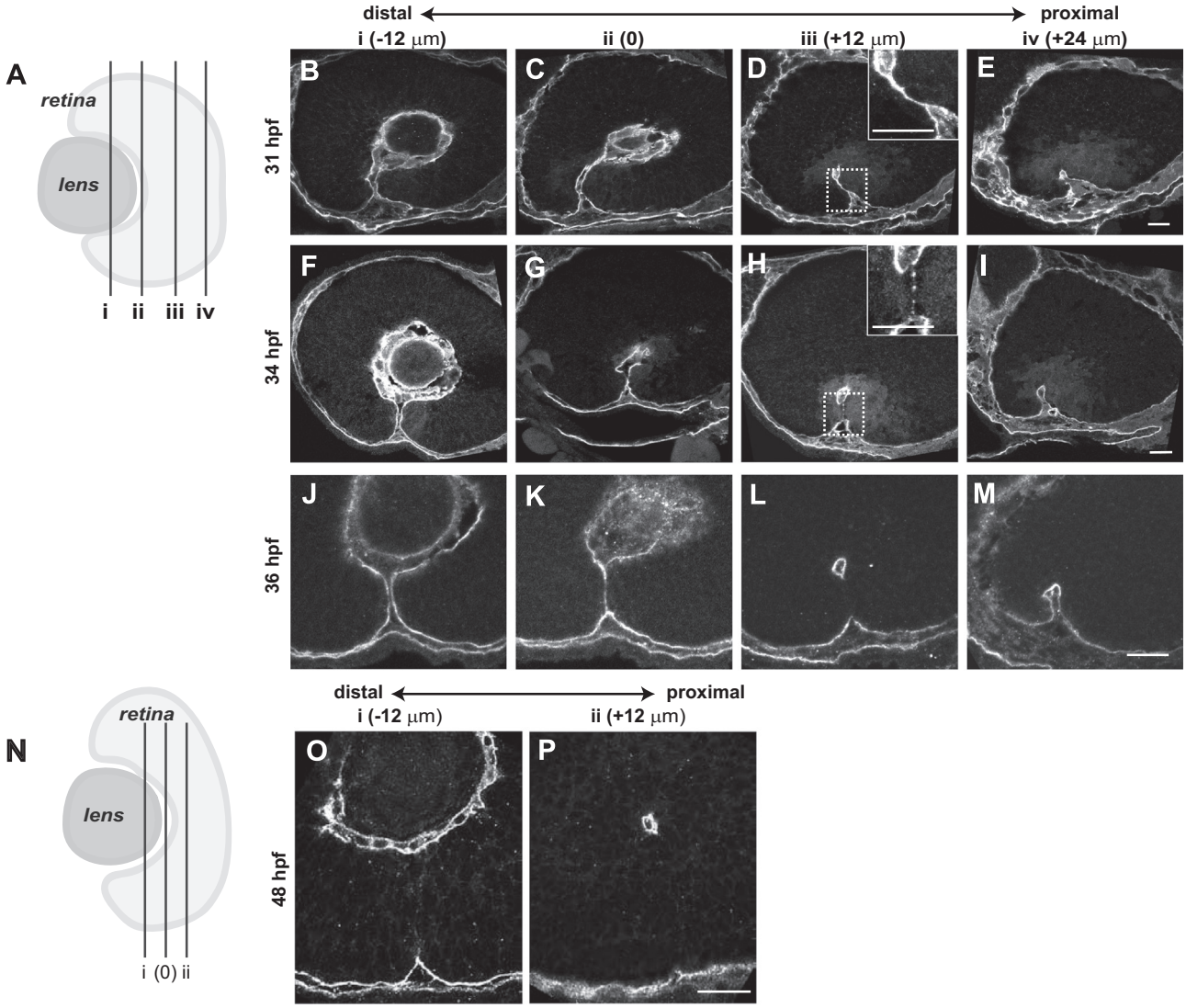

Fig. 1. Temporal and spatial dynamics of basement membrane breakdown during choroid fissure closure in zebrafish. (A) Schematic depicting the approximate level of sections in B-M along the proximal-distal axis of the CF. The vitreous cavity was defined as central, and sections were taken at 12 μm intervals proximally and distally from this point. (B-M) Sagittal sections along the proximal-distal axis of the retina, immunostained for Lam-111 expression. (B-E) 31 hpf, (F-I) 34 hpf, (J-M) 36 hpf. Insets in D, H show high magnification views of the regions in the dashed boxes. (N) Schematic depicting the plane of section for 48 hpf embryos in O,P. (O,P) Representative sagittal sections along the proximal-distal axis of the retina immunostained for Lam-111. Scale bars = 20 μm.

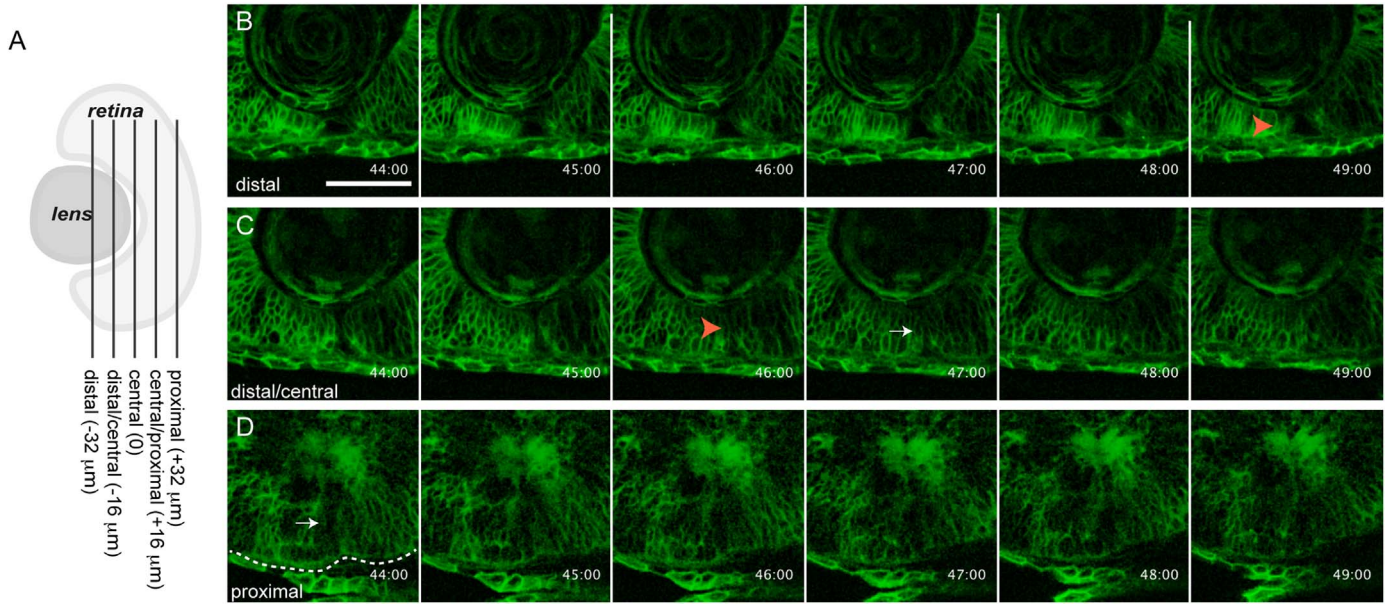

Fig. 2. *in vivo* imaging of choroid fissure closure in zebrafish. (A) Schematic depicting the approximate level of sections in B-D along the proximal-distal axis of the CF. The vitreous cavity was defined as central, and optical sections were taken at 16 μm intervals proximally and distally from this point. (B-D) *membrane-GFP* injected embryos were imaged throughout the CF. Single micron optical slices are shown from 44 to 49 hpf and at three distinct proximal-distal regions of the CF. (B) Distally, the CF remains open until at least 49 hpf. (C) Distal/centrally, the CF appears to close between 46–47 hpf. (D) Proximally, the CF already appears to be closed at 44 hpf. Orange arrowheads in B,C mark open CF. White arrow in C marks what appears to be a closed CF. Dashed line outlines the RPE. Scale bar = 50 μm.

3.2. Temporal and spatial dynamics of tissue fusion during CF closure

Next, we wanted to determine when tissue fusion occurs during CFC and we turned to *in vivo* imaging to address this question. Embryos were injected with *membrane-GFP* (Fig. 2) or *utrophin-GFP* (data not shown) mRNA at the one-cell stage and embryos were imaged at various proximal-distal positions throughout the CF over time. Our initial imaging strategy focused on 24–40 hpf embryos, hypothesizing that fusion would likely occur between ~32 and 34 hpf, correlating closely with basement membrane breakdown. However, during this time frame, fusion appeared to begin only at the very end of the imaging window (*data not shown*). Thus, we shifted our imaging window slightly later, to 32–52 hpf, to better observe the initiation and completion of CFC (Fig. 2A; n = 4 embryos; Supplemental Movies 1–3). As above, for axial orientation along the proximal-distal axis we again designated the central CF as the vitreous cavity; however, because there is substantial growth and morphogenesis occurring in the eye over these time points, and because we did not utilize a lineage marker to track individual cells, it is not possible to directly compare the locations of CF cells from early time points (i.e. BM breakdown assays) to later time points analyzed in these fusion assays. From the time-lapse movies, fusion of the CF in the most proximal regions imaged appeared to initiate at ~37.5 hpf and to be complete by 44 hpf, based on the tight apposition between the two sides of the CF and the appearance of a seemingly continuous RPE (Fig. 2D). In the distal/central CF, the two sides of the CF became tightly apposed at ~46 and 47 hpf (Fig. 2C), while in the most distal CF, fusion had yet to begin even at 49 hpf (Fig. 2B).

Supplementary material related to this article can be found online at http://dx.doi.org/10.1016/j.ydbio.2016.09.008.

Absence of Lam-111 staining in the central CF and the tight apposition of the sides of the CF at 36 hpf (Fig. 1L) initially suggested that tissue fusion might occur immediately after BM breakdown; however, *in vivo* imaging data indicated a significantly later timing for the fusion process. To address this apparent contradiction, we performed immunohistochemistry on sagittal sections taken at 16 μm intervals along the proximal-distal axis of the CF, identifying the margins of CF cells with phalloidin, which marks F-actin, and adherens junctions with β-catenin immunohistochemistry (Fig. 3). Co-localization of F-actin and β-catenin provides a reliable indication that a stable adherens junction had formed, and thus, that fusion had occurred (Gumbiner, 2000; Halbleib and Nelson, 2006; Hartsock and Nelson, 2008; Oda and Takeichi, 2011). Examining single 1 μm optical sections at 44 hpf revealed that F-actin and β-catenin were co-localized in the central/proximal region of the CF, indicating that the CF was indeed fused at this time (Fig. 3D). Proximal to this however, the CF was still open at 44 hpf (Fig. 3E), despite *in vivo* imaging data that indicated the two sides of the CF might already have undergone fusion (Fig. 2). Tissue fusion proceeded bi-directionally from the central/proximal region, with F-actin and β-catenin co-localization in the central (Fig. 3M) and proximal (Fig. 3O) aspects of the CF at ~47 hpf (Fig. 3M), and the distal/central CF at 49 hpf (Fig. 3Q). Fusion is complete by ~54 hpf in most embryos, with the exception of the most distal CF, which is fully closed by 72 hpf (*data not shown*). At all regions of fusion, F-actin and β-catenin formed a "seam" at the site of fusion (e.g. Fig. 3M), which then dissipated within 1–2 h thereafter (e.g. Fig. 3R). Previously, in cell culture it was observed that there are areas of organized actin outside of the apical zonula adherens that are required for proper contractile activity (Wu et al., 2014). Examination of the CF in each single 1 μm optical slice through an individual 16 μm section plane revealed a progressive co-localization between F-actin and β-catenin within the CF where there are points in which β-catenin is present without F-actin and *vice versa*, indicating that both the traditional apical cortical ring (seam) and lateral adhesion clusters (puncta) are present in CF cells during CF fusion (Fig. 3U).

3.3. Periocular mesenchyme-derived endothelial cells contribute to CFC

TEM studies in mouse have shown that BM breakdown correlates with a population of "amoeboid phagocytic cells" present in the CF, and these cells possess pseudopodia which adhere to the BM at regions where it is being actively degraded (Hero, 1990;

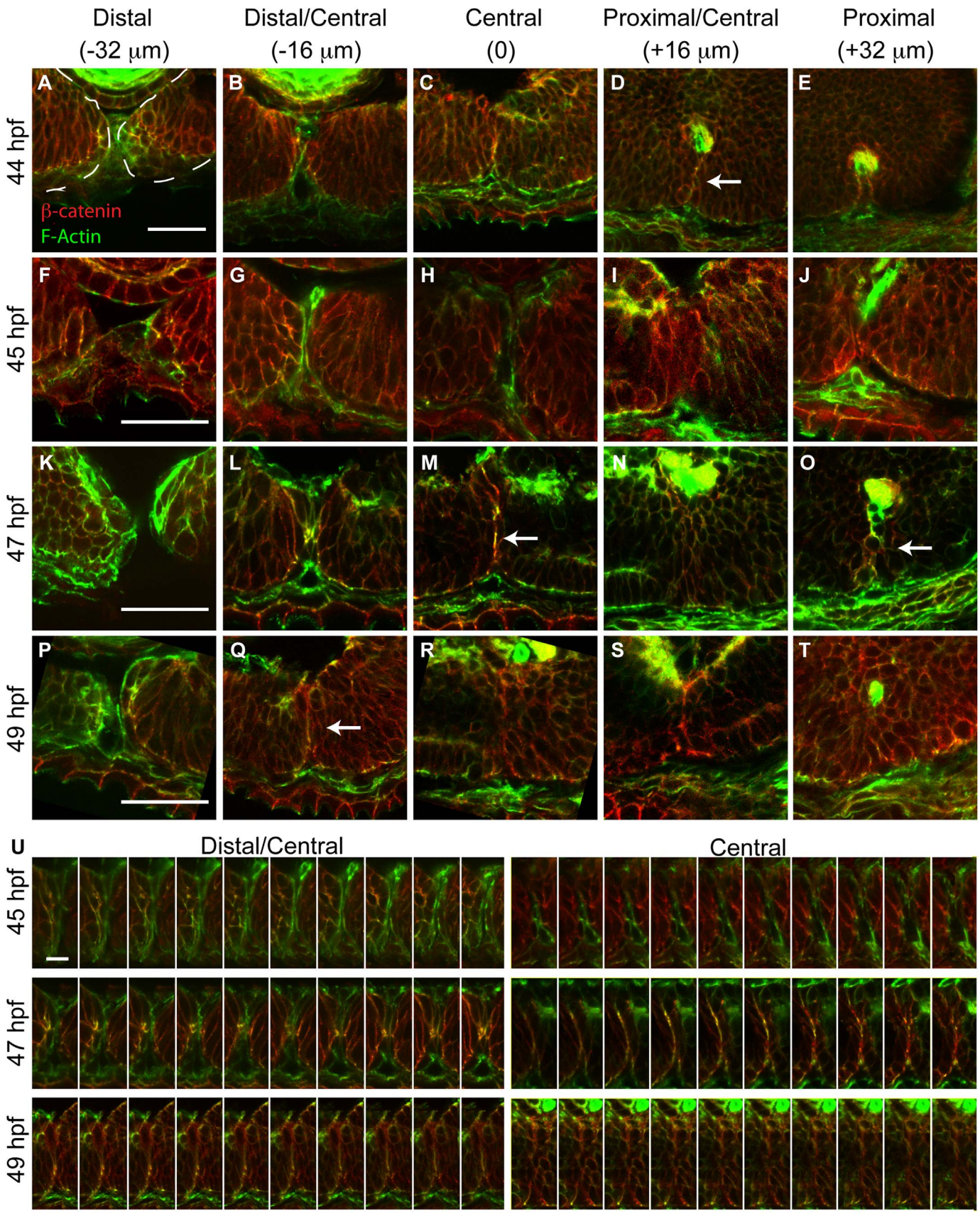

Fig. 3. Temporal and spatial dynamics of tissue fusion during choroid fissure closure in zebrafish. Single micron optical sections from sagittal cryosections stained with phalloidin (green) and anti-β-catenin (red) at distinct proximal-distal regions of the CF over time. As in Fig. 2, the vitreous cavity was defined as central, and sections were taken at 16 μm intervals proximally and distally from this point. (A-E) At 44 hpf, the CF is fused in central/proximal sections (white arrow) based on co-localization between F-actin and β-catenin in a fusion 'seam'. (F-J) At 45 hpf, the two sides of the CF are tightly apposed but no fusion outside of the central-proximal region is detected. (K-O) At 47 hpf, a fusion seam is present within central and proximal sections, and there are punctate regions of co-localization in distal/central sections. (P-T) At 49 hpf, the fusion seam has disappeared in the central and proximal CF regions while it is appearing in the distal/central region. (U) Single 1 μm optical sections from one section plane aligned distal (left) to proximal (right) demonstrate a progressive co-localization of F-actin and β-catenin in the CF and formation of the fusion seam. Scale bar = 50 μm (A-T) and 5 μm (U).

Hero et al., 1991). In Mitf$^{-/-}$ mutants, there is a decrease or complete absence of these phagocytic cells in CF regions where BM breakdown did not occur. Based on these observations, the authors hypothesized that these phagocytic cells were of mesenchymal origin and that they contribute to BM breakdown. Periocular mesenchyme (POM) cells migrate into the developing eye to form a variety of ocular and extraocular structures (Gage et al., 2005). Moreover, POM cells have been reported to function during CFC in a variety of contexts, and in a variety of model systems, with defects in POM function or survival resulting in colobomas (Evans and Gage, 2005; Kim et al., 2007; McMahon et al., 2009; See and Clagett-Dame, 2009; Bajpai et al., 2010; Lupo et al., 2011). Despite these studies, the cellular mechanisms through which POM cells contribute to CFC remain largely unknown.

We hypothesized that POM might play a direct role in mediating CFC. To test this hypothesis, we utilized transgenic zebrafish lines in which GFP is expressed in distinct populations of POM cells. Tg(*sox10:*eGFP) expresses GFP in neural crest cells (Wada et al., 2005); during CFC, *sox10:*GFP^{+} cells were detected transiently in the CF, but not in regions where BM breakdown was occurring and were no longer present within the CF at 37 hpf (Fig. 4A-A″; Fig. S1A-A″). In the eye, subsets of POM cells migrate through the CF to generate the hyaloid vasculature, and these are labeled in Tg(*fli1a:*eGFP) embryos (Lawson and Weinstein, 2002; Alvarez et al., 2007; Hartsock et al., 2014). In comparison to *sox10:* GFP^{+} cells, which rapidly transit the CF to enter the anterior chamber, *fli1a:*eGFP^{+} cells are retained in the CF to generate the hyaloid. Moreover, observing *kdrl:*mCherry^{+} hyaloid cells in *membrane-GFP* injected embryos highlights that hyaloid cells are retained in the CF as late as 40 hpf (Supplemental Movie 4). Interestingly, *fli1a:*eGFP^{+} cells localized to regions of the CF where the BM was absent or was punctate (Fig. 4B,C; Fig. S1B-E), and they possessed pronounced F-actin accumulations that localize to regions of BM breakdown (Fig. 4C-C‴).

Supplementary material related to this article can be found online at http://dx.doi.org/10.1016/j.ydbio.2016.09.008.

3.4. POM is required for basement membrane breakdown during choroid fissure closure

The data presented thus far support a model in which POM cells could play a role during CFC, possibly utilizing an F-actin dependent process to facilitate BM breakdown. To test this model, we analyzed Talin function during CFC. Talin is a scaffold protein that links integrins to the actin cytoskeleton, playing a critical role in integrin activation (Legate and Fassler, 2009; Moser et al., 2009; Desiniotis and Kyprianou, 2011). In zebrafish, *talin1* is enriched in the CF, in both POM cells lining the CF and retinal/RPE cells that comprise the fissure (Fig. 5A, D-F). A *talin1* loss of function mutant was previously identified, but its role during eye development has not yet been examined (Amsterdam et al., 2004). *tln1*^{hi3093} mutants possessed colobomas at 3 dpf (Fig. 5B,C), with the distal aspect of the CF more affected, reminiscent of an iris coloboma in humans (Chang et al., 2006). BM degradation in the CF of *tln1* mutants was deficient at 48 hpf, a time point at which BM degradation was complete in most CF regions of phenotypically wild-type siblings (Fig. 5G-J). Distribution of *talin1* in the POM and retinal/RPE cells within the CF, and correlation between *fli1a:*eGFP

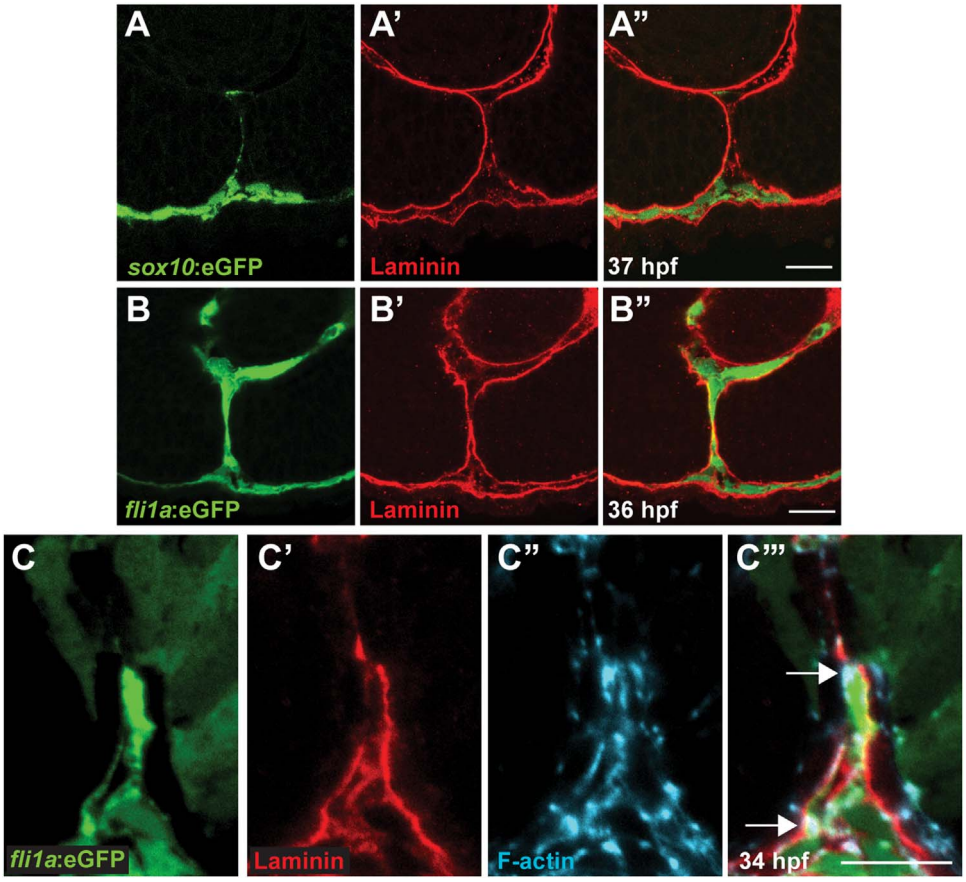

Fig. 4. Periocular mesenchymal cells contribute to CFC. (A-C) Sagittal views of the CF stained with anti-GFP (green), Lam-111 (red) and/or phalloidin (blue). (A) Few *sox10:* eGFP^{+} cells are detected in the CF, 37 hpf section pictured. (B) *fli1a:*eGFP^{+} cells are retained in the CF. 36 hpf section pictured. (C) *fli1a:*eGFP^{+} cells possess F-actin accumulations that localize to regions of BM breakdown. Arrows denote puncta of F-actin where Lam-111 is low or absent. 34 hpf section pictured. Scale bar = 20 μm (A,B) and 10 μm (C).

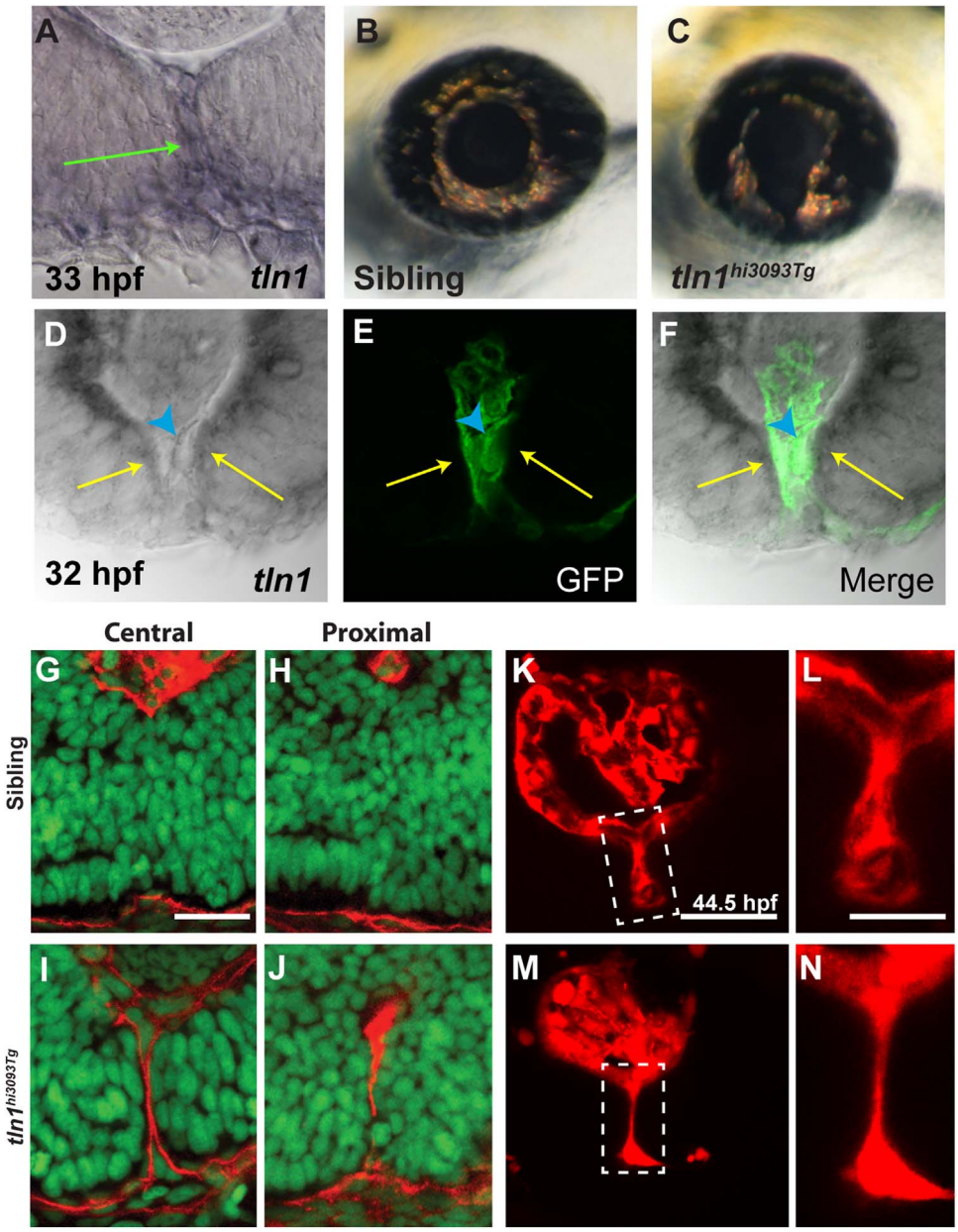

Fig. 5. talin1 is required for CFC in zebrafish. (A) *talin1* is expressed within the POM and retinal/RPE cells lining the CF at 33 hpf (arrow). (B,C) Lateral views of the eye of *tln1*^{hi3093Tg} mutant (C) and wild-type sibling (B) at 3dpf. *tln1* mutants possess colobomas. (D-F) Distal section through the eye of a 32 hpf embryo demonstrating *talin1* expression within the retina/RPE cells lining the CF (arrows) and the hyaloid vasculature (marked by GFP expression from *fli1a*:eGFP; arrowhead). (G-J) Sagittal sections through the eyes of 48 hpf *tln1* mutants and siblings stained with Lam-111 (red) and Sytox-green (DNA; green). BM degradation is disrupted in *tln1* mutants at 48 hpf. (K-N) Maximum projection images of the distal hyaloid in *tln1* mutants and siblings demonstrating severe hypotrophy of the hyaloid in the *tln1* mutant at 44.5 hpf. Scale bar=20 μm (G-J, K,M) and 50 μm (L,N).

expressing cells and regions of BM breakdown indicated that the POM-derived hyaloid vasculature might be affected in *tln1* mutants. To assess hyaloid formation we crossed the *kdrl: mCherry* transgene into the *tln1* mutant line and imaged the hyaloid as previously described (Hartsock et al., 2014). Indeed, the structure of the hyaloid was disrupted in the distal/central region of the CF with the hyaloid severely hypotrophic relative to that in wild-type siblings (Fig. 5K-N).

These findings support a model in which BM breakdown during CFC requires an actin-mediated process and indicate that POM-derived endothelial cells and/or the hyaloid itself may play a direct role in facilitating BM breakdown. To test this model we utilized the *cloche* mutant which lacks all early ocular vasculature (Stainier et al., 1995; Liao et al., 1997; Dhakal et al., 2015), thus eliminating any potential contribution of POM-derived endothelial cells to CFC. As in *tln1* mutants, BM degradation was deficient in *cloche* mutants and Lam-111 staining was detected in both proximal and distal regions of the CF at 51 hpf (Fig. 6C,D), a time at which it is absent from wild-type siblings (Fig. 6A,B). Lam-111 staining was absent in *cloche* mutants by 3dpf (data not shown) however, indicating that the absence of the hyaloid vasculature delayed, but did not completely prevent, BM breakdown.

4. Discussion

The molecular and cellular underpinnings of CFC are largely unknown, despite the relatively high incidences of colobomas in the human population and the increasing number of identified loci associated with isolated or syndromic colobomas (e.g. Graw, 2003;

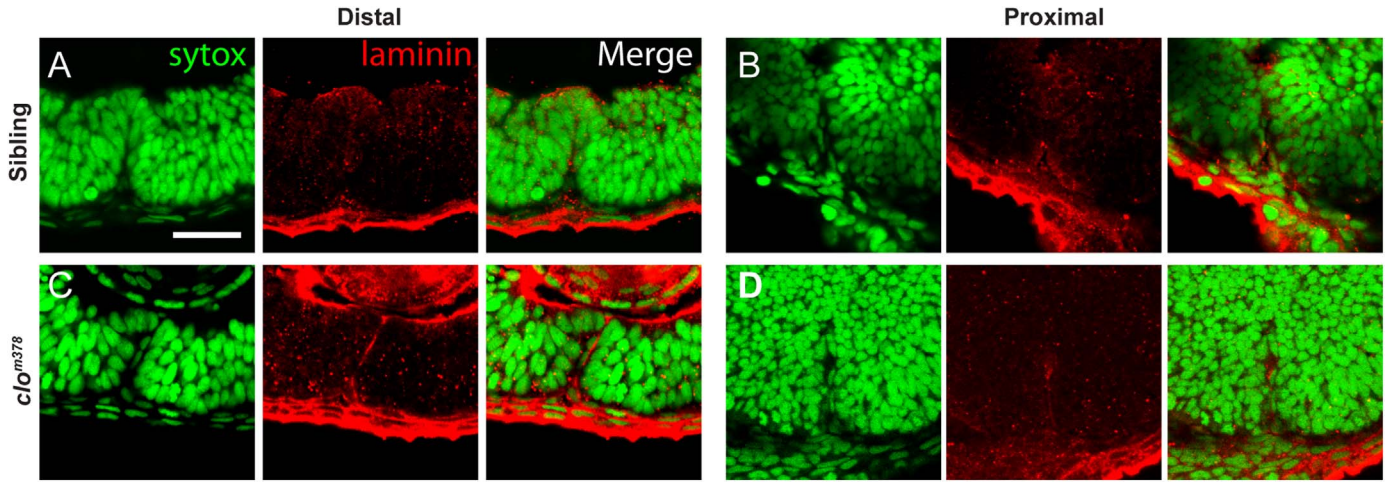

Fig. 6. POM-derived endothelial cells facilitate BM breakdown during CFC. (A-D) Sagittal sections through the eyes of 51 hpf *cloche*^{m378} mutants and siblings stained with Lam-111 (red) and Sytox-green (DNA; green). BM degradation is disrupted in *cloche*^{m378} mutants in both the (C) proximal and (D) distal regions of the CF when compared to (A,B) siblings. Scale bar=25 μm.

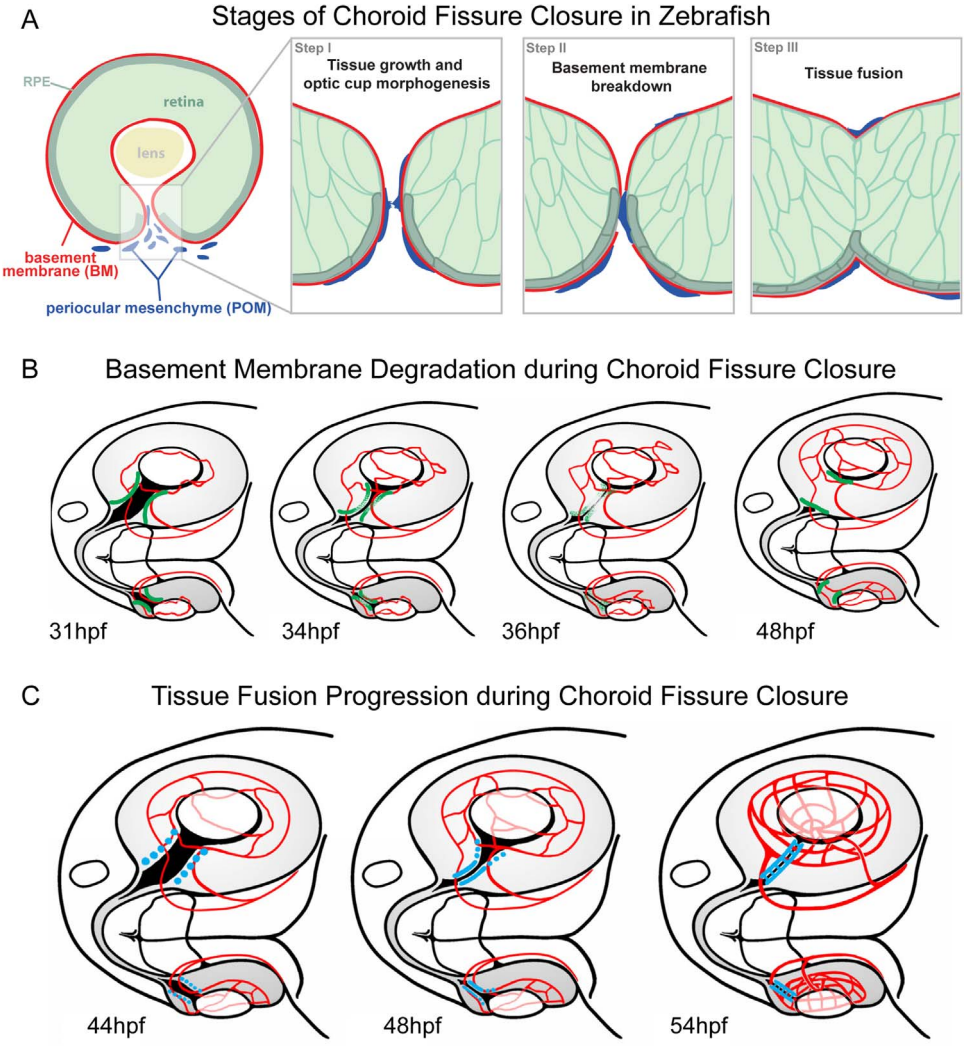

Fig. 7. Schematics depicting key stages and events of CFC. (A) During Stage I, tissue growth and optic cup morphogenesis generates an appropriate number of cells, which are correctly patterned and positioned in the optic cup. The opposing sides of the CF become closely apposed. During Stage II, the basement membrane lining the CF is degraded through a process involving periocular mesenchyme cells. During Stage III, tissue fusion between opposing sides of the CF closes the fissure. (B) Schematic of basement membrane breakdown (green=BM) within the CF from 31 to 48 hpf. BM breakdown initiates in the central/proximal CF and proceeds bi-directionally, being complete by 48 hpf except in the most distal regions of the CF. (C) Schematic of tissue fusion (blue=fusion) in the CF from 41 to 54 hpf. The hyaloid vasculature is depicted in red in each image. Fusion initiates in the central/proximal CF and proceeds bi-directionally, being complete by ~54 hpf except in the most distal regions of the CF.

Please cite this article as: James, A., et al., (2016), http://dx.doi.org/10.1016/j.ydbio.2016.09.008

Gregory-Evans et al., 2004; Fitzpatrick and van Heyningen, 2005; Chang et al., 2006). CFC can be segregated into three principal stages (Fig. 7A). During Stage I, optic cup morphogenesis proceeds such that the correct number of cells is generated, and the retina/RPE aspects of the CF properly develop and become positioned in the ventral aspect of the optic cup. Stage II of CFC involves breakdown of the basement membrane/basal lamina lining the neuroepithelial and RPE components of the CF. Stage III is comprised of tissue fusion events that serve to close the CF. Many genes mutated in human coloboma patients have been shown to mechanistically function during Stage I when examined in animal model systems; these include *SALL2* (Kelberman et al., 2014), *PAX2* (Sanyanusin et al., 1995; Torres et al., 1996; Macdonald et al., 1997; Bower et al., 2012), CHD7 (Bosman et al., 2005; Lalani et al., 2006; Bajpai et al., 2010), and *GDF3* and *GDF6* (Asai-Coakwell et al., 2007; Ye et al., 2010). Moreover, *in vivo* imaging studies have also begun to identify cell movements and cell populations that generate distinct components of the CF (Picker et al., 2009). By comparison, virtually nothing is known about the mechanisms underlying the Stage II BM breakdown or Stage III tissue fusion events of CFC. Here, we have utilized zebrafish to determine the spatial and temporal characteristics of BM breakdown (Fig. 7B) and tissue fusion (Fig. 7C) and thereby provide a model in which the cellular and molecular underpinnings of these processes can now be elucidated.

Previous studies in a variety of model systems have led to the hypothesis that defects in Stage II, an inability to degrade the CF BM, result in colobomas. Indeed, knockout or loss of function mutations in *Pax2/pax2* (Torres et al., 1996; Macdonald et al., 1997) and *Vax2* (Barbieri et al., 2002) result in retention of the CF BM and colobomas. Similarly, in Fatty Liver Shionogi mice, the CF BM is retained and colobomas result (Tsuji et al., 2012). These data lead to a model in which BM breakdown is required for normal CFC; however there is very little known about how this process occurs *in vivo*. As discussed above, TEM studies in mouse have shown that BM breakdown correlates with a population of cells that are possibly mesenchymal in origin (Hero, 1990; Hero et al., 1991). POM cells, comprised of lateral plate mesenchyme and cranial neural crest derivatives, migrate into the developing eye to form a variety of ocular and extraocular structures (Gage et al., 2005; Williams and Bohnsack, 2015). POM cells are known to be required for CFC, with defects in *lmx1b*, *Tfap2a*/*tfap2a, foxc1*, *nlz1* and *Pitx2*/*pitx2* resulting in colobomas (Gage et al., 1999; Brown et al., 2009; Gestri et al., 2009; McMahon et al., 2009; Bassett et al., 2010; Lupo et al., 2011). Retinoic acid (RA) signaling also contributes to CFC, by acting both directly on the ventral optic cup, as well as regulating gene expression within the POM (Lupo et al., 2011). Indeed, defects in RA signaling have been shown to cause a reduction in *Pitx2* expression in the POM, resulting in retention of the BM lining the CF and colobomas (See and Clagett-Dame, 2009).

Of particular interest are the POM-derived endothelial cells that migrate through the CF and into the vitreous to form the hyaloid (Saint-Geniez and D'Amore, 2004; Alvarez et al., 2007; Hartsock et al., 2014). Our data demonstrate that regions of BM breakdown correlate with actin enrichment in POM cells within the CF and that these cells are likely POM-derived endothelial cells that express *fli1a*-driven transgenes and give rise to the hyaloid vasculature (Fig. 4). Roles for endothelial cells during tissue morphogenesis have been identified in the developing liver; for example, endothelial cells are required for hepatic outgrowth, acting prior to the formation of functional vessels (Matsumoto et al., 2001), and they influence the apical-basal polarity of developing hepatocytes (Sakaguchi et al., 2008).

We identified actin enrichment in POM cells coincident with areas of BM degradation (Fig. 4), and, when combined with the classic TEM studies of Isabelle Hero (Hero, 1990; Hero et al., 1991), we hypothesized that POM cells actively degrade the CF BM as they transit through the CF. We examined BM breakdown in *talin1* and *cloche* mutants (Figs. 5, 6). *talin1* encodes a scaffold protein linking integrins to the actin cytoskeleton, but little is known about function during eye development. *cloche* mutants lack all POM-derived ocular vasculature but surprisingly, despite being microphthalmic, the early phases of eye development are fairly normal in *cloche*, with pronounced retinal defects not detectable until after 48 hpf, well beyond the window for BM breakdown in most of the CF (Dhakal et al., 2015). Both mutants possessed defects in BM breakdown (Figs. 5, 6), thus supporting a model in which POM-derived endothelial cells and/or the hyaloid vasculature itself, facilitate BM breakdown during CFC. Notably, BM breakdown was delayed, but did eventually complete in *cloche* mutants. These data suggest that the ocular vasculature is not the only cell or tissue type required for BM breakdown and that there is likely a hyaloid-independent component to BM breakdown. When compared to *cloche*, the more severe BM breakdown and coloboma phenotypes in *tln1* mutants also suggest that whatever cell or tissue type is required for efficient BM breakdown, it is likely to do so in an actin-dependent fashion. The TEM studies of Hero noted cellular protrusions from retinal cells in the CF that correlated with regions of BM breakdown (Hero, 1990) and thus, it is possible that retinal and/or RPE components of the CF also participate in BM breakdown and fill such a role in *cloche* mutants. Mechanistically, podosomes and invadosomes are known to mediate focal BM breakdown in a variety of developmental and cell biological contexts, including endothelial cells (Murphy and Courtneidge, 2011; van den Dries et al., 2014) making them interesting candidates for further analysis. Future studies will examine the BM breakdown and CFC phenotypes in loss-of function mutants for podosome/invadosome components like *tks4/sh3pxd2, mmp2 and mmp14*.

With respect to tissue fusion during CFC (Stage III), several gene products have been identified that are required for fusion in the CF, but the mechanisms underlying the fusion process are not yet clear (Erdmann et al., 2003; Masai et al., 2003; Chen et al., 2012). In addition to defects arising from loss of function of retinal genes, disruptions to RPE specification and differentiation have also been shown to result in colobomas. For example, disruption of Mitf or an RPE-specific loss of β-catenin produces colobomas during mouse eye development (Scholtz and Chan, 1987; Westenskow et al., 2009), supporting the idea that the RPE also contributes to CFC. CFC defects arising in these models are thought to result from early Stage I defects in which overall optic cup development is perturbed, but it is also possible that CFC defects reflect a role for the RPE in tissue fusion itself. As in mouse and hamster (Geeraets, 1976; Hero, 1990; Hero et al., 1991), the RPE is inverted into the CF during the early stages of CFC in zebrafish (Fig. 3 and *data now shown*) supporting a potential role in mediating fusion.

Through *in vivo* imaging, F-actin staining and β-catenin immunohistochemistry, we determined the spatial and temporal characteristics of tissue fusion in zebrafish. While *in vivo* time lapse imaging provided a general indication to the timing of CFC, β-catenin immunohistochemistry provided a more accurate molecular readout of fusion between the tightly apposed sides of the CF. Given the transient enrichment of β-catenin at regions of nascent adhesion, cadherin-mediated mechanisms are likely to be involved in CF fusion. Indeed, multiple *N-cadherin* mutants exist in zebrafish that present with colobomas (Liu et al., 2001; Erdmann et al., 2003; Masai et al., 2003) although the cell biological mechanisms leading to these defects have not yet been resolved. Other cadherins expressed in the zebrafish eye include R-cadherin (Liu et al., 1999a, 1999b; Babb et al., 2005), cadherin 6 (Liu et al., 2008), and protocadherin 9 and 17 (Liu et al., 2009; Chen et al., 2013b), and these could also play a role in tissue fusion during CFC.

Please cite this article as: James, A., et al., (2016), http://dx.doi.org/10.1016/j.ydbio.2016.09.008

Finally, the rapid turnover of β-catenin within the CF presents an excellent model to study how formation and maintenance of adherens junctions are regulated *in vivo*.

Acknowledgements

We are grateful to Jeff Essner for *kdrl*:mCherry and *kdrl*:moesin-GFP transgenics, Beth Roman for *cloche*, Adam Kwiatkowski for providing antibodies, members of the Gross lab for helpful suggestions and comments on this work, and Roky Erickson for technical support. This work was supported by a CAREER Award from the National Science Foundation (IOS-0745782), grants from the National Eye Institute (RO1-EY18005 to JMG, and F32-EY23910 to AH), and NIH CORE Grant P30 EY08098 to the Department of Ophthalmology. *In vivo* imaging was performed on a confocal microscope funded by NIH S10-RR028951. Zebrafish were obtained from ZIRC, which is supported by NIH-NCRR Grant P40 RR012546. We acknowledge additional support from the Eye and Ear Foundation of Pittsburgh and from an unrestricted grant from Research to Prevent Blindness, New York, NY.

Appendix A. Supplementary material

Supplementary data associated with this article can be found in the online version at http://dx.doi.org/10.1016/j.ydbio.2016.09.008.

References

Alvarez, Y., Cederlund, M.L., Cottell, D.C., Bill, B.R., Ekker, S.C., Torres-Vazquez, J., Weinstein, B.M., Hyde, D.R., Vihtelic, T.S., Kennedy, B.N., 2007. Genetic determinants of hyaloid and retinal vasculature in zebrafish. BMC Dev. Biol. 7, 114.

Amsterdam, A., Nissen, R.M., Sun, Z., Swindell, E.C., Farrington, S., Hopkins, N., 2004. Identification of 315 genes essential for early zebrafish development. Proc. Natl. Acad. Sci. USA 101 (35), 12792–12797.

Asai-Coakwell, M., French, C.R., Berry, K.M., Ye, M., Koss, R., Somerville, M., Mueller, R., van Heyningen, V., Waskiewicz, A.J., Lehmann, O.J., 2007. GDF6, a novel locus for a spectrum of ocular developmental anomalies. Am. J. Hum. Genet. 80 (2), 306–315.

Atkinson-Leadbeater, K., Hehr, C.L., McFarlane, S., 2014. Fgfr signaling is required as the early eye field forms to promote later patterning and morphogenesis of the eye. Dev. Dyn.: Off. Publ. Am. Assoc. Anat. 243 (5), 663–675.

Babb, S.G., Kotradi, S.M., Shah, B., Chiappini-Williamson, C., Bell, L.N., Schmeiser, G., Chen, E., Liu, Q., Marrs, J.A., 2005. Zebrafish R-cadherin (Cdh4) controls visual system development and differentiation. Dev. Dyn.: Off. Publ. Am. Assoc. Anat. 233 (3), 930–945.

Bajpai, R., Chen, D.A., Rada-Iglesias, A., Zhang, J., Xiong, Y., Helms, J., Chang, C.P., Zhao, Y., Swigut, T., Wysocka, J., 2010. CHD7 cooperates with PBAF to control multipotent neural crest formation. Nature 463 (7283), 958–962.

Bar-Yosef, U., Abuelaish, I., Harel, T., Hendler, N., Ofir, R., Birk, O.S., 2004. CHX10 mutations cause non-syndromic microphthalmia/ anophthalmia in Arab and Jewish kindreds. Hum. Genet. 115 (4), 302–309.

Barbieri, A.M., Broccoli, V., Bovolenta, P., Alfano, G., Marchitiello, A., Mocchetti, C., Crippa, L., Bulfone, A., Marigo, V., Ballabio, A., et al., 2002. Vax2 inactivation in mouse determines alteration of the eye dorsal-ventral axis, misrouting of the optic fibres and eye coloboma. Development 129 (3), 805–813.

Bassett, E.A., Williams, T., Zacharias, A.L., Gage, P.J., Fuhrmann, S., West-Mays, J.A., 2010. AP-2alpha knockout mice exhibit optic cup patterning defects and failure of optic stalk morphogenesis. Hum. Mol. Genet. 19 (9), 1791–1804.

Bermejo, E., Martinez-Frias, M.L., 1998. Congenital eye malformations: clinical-epidemiological analysis of 1,124,654 consecutive births in Spain. Am. J. Med. Genet. 75 (5), 497–504.

Bibliowicz, J., Tittle, R.K., Gross, J.M., 2011. Toward a better understanding of human eye disease insights from the zebrafish, Danio rerio. Prog. Mol. Biol. Transl. Sci. 100, 287–330.

Bosman, E.A., Penn, A.C., Ambrose, J.C., Kettleborough, R., Stemple, D.L., Steel, K.P., 2005. Multiple mutations in mouse Chd7 provide models for CHARGE syndrome. Hum. Mol. Genet. 14 (22), 3463–3476.

Bower, M., Salomon, R., Allanson, J., Antignac, C., Benedicenti, F., Benetti, E., Binenbaum, G., Jensen, U.B., Cochat, P., DeCramer, S., et al., 2012. Update of PAX2 mutations in renal coloboma syndrome and establishment of a locus-specific database. Hum. Mutat. 33 (3), 457–466.

Brown, J.D., Dutta, S., Bharti, K., Bonner, R.F., Munson, P.J., Dawid, I.B., Akhtar, A.L., Onojafe, I.F., Alur, R.P., Gross, J.M., et al., 2009. Expression profiling during ocular development identifies 2 Nlz genes with a critical role in optic fissure closure. Proc. Natl. Acad. Sci. USA 106 (5), 1462–1467.

Burkel, B.M., von Dassow, G., Bement, W.M., 2007. Versatile fluorescent probes for actin filaments based on the actin-binding domain of utrophin. Cell Motil. Cytoskelet. 64 (11), 822–832.

Cai, Z., Tao, C., Li, H., Ladher, R., Gotoh, N., Feng, G.S., Wang, F., Zhang, X., 2013. Deficient FGF signaling causes optic nerve dysgenesis and ocular coloboma. Development 140 (13), 2711–2723.

Chang, L., Blain, D., Bertuzzi, S., Brooks, B.P., 2006. Uveal coloboma: clinical and basic science update. Curr. Opin. Ophthalmol. 17 (5), 447–470.

Chen, S., Lewis, B., Moran, A., Xie, T., 2012. Cadherin-mediated cell adhesion is critical for the closing of the mouse optic fissure. PLoS One 7 (12), e51705.

Chen, S., Li, H., Gaudenz, K., Paulson, A., Guo, F., Trimble, R., Peak, A., Seidel, C., Deng, C., Furuta, Y., et al., 2013a. Defective FGF signaling causes coloboma formation and disrupts retinal neurogenesis. Cell Res. 23 (2), 254–273.

Chen, Y., Londraville, R., Brickner, S., El-Shaar, L., Fankhauser, K., Dearth, C., Fulton, L., Sochacka, A., Bhattarai, S., Marrs, J.A., et al., 2013b. Protocadherin-17 function in Zebrafish retinal development. Dev. Neurobiol. 73 (4), 259–273.

Deml, B., Kariminejad, A., Borujerdi, R.H., Muheisen, S., Reis, L.M., Semina, E.V., 2015. Mutations in MAB21L2 result in ocular Coloboma, microcornea and cataracts. PLoS Genet. 11 (2), e1005002.

Desiniotis, A., Kyprianou, N., 2011. Significance of talin in cancer progression and metastasis. Int. Rev. Cell Mol. Biol. 289, 117–147.

Dhakal, S., Stevens, C.B., Sebbagh, M., Weiss, O., Frey, R.A., Adamson, S., Shelden, E. A., Inbal, A., Stenkamp, D.L., 2015. Abnormal retinal development in Cloche mutant zebrafish. Dev. Dyn.: Off. Publ. Am. Assoc. Anat. 244 (11), 1439–1455.

Erdmann, B., Kirsch, F.P., Rathjen, F.G., More, M.I., 2003. N-cadherin is essential for retinal lamination in the zebrafish. Dev. Dyn.: Off. Publ. Am. Assoc. Anat. 226 (3), 570–577.

Evans, A.L., Gage, P.J., 2005. Expression of the homeobox gene Pitx2 in neural crest is required for optic stalk and ocular anterior segment development. Hum. Mol. Genet. 14 (22), 3347–3359.

Fitzpatrick, D.R., van Heyningen, V., 2005. Developmental eye disorders. Curr. Opin. Genet. Dev. 15 (3), 348–353.

Gage, P.J., Rhoades, W., Prucka, S.K., Hjalt, T., 2005. Fate maps of neural crest and mesoderm in the mammalian eye. Invest. Ophthalmol. Vis. Sci. 46 (11), 4200–4208.

Gage, P.J., Suh, H., Camper, S.A., 1999. Dosage requirement of Pitx2 for development of multiple organs. Development 126 (20), 4643–4651.

Geeraets, R., 1976. An electron microscopic study of the closure of the optic fissure in the golden hamster. Am. J. Anat. 145 (4), 411–431.

Gestri, G., Link, B.A., Neuhauss, S.C., 2012. The visual system of zebrafish and its use to model human ocular diseases. Dev. Neurobiol. 72 (3), 302–327.

Gestri, G., Osborne, R.J., Wyatt, A.W., Gerrelli, D., Gribble, S., Stewart, H., Fryer, A., Bunyan, D.J., Prescott, K., Collin, J.R., et al., 2009. Reduced TFAP2A function causes variable optic fissure closure and retinal defects and sensitizes eye development to mutations in other morphogenetic regulators. Hum. Genet. 126 (6), 791–803.

Graw, J., 2003. The genetic and molecular basis of congenital eye defects. Nat. Rev. Genet. 4 (11), 876–888.

Gregory-Evans, C.Y., Williams, M.J., Halford, S., Gregory-Evans, K., 2004. Ocular coloboma: a reassessment in the age of molecular neuroscience. J. Med. Genet. 41 (12), 881–891.

Gumbiner, B.M., 2000. Regulation of cadherin adhesive activity. J. Cell Biol. 148 (3), 399–404.

Halbleib, J.M., Nelson, W.J., 2006. Cadherins in development: cell adhesion, sorting, and tissue morphogenesis. Genes Dev. 20 (23), 3199–3214.

Hartsock, A., Lee, C., Arnold, V., Gross, J.M., 2014. In vivo analysis of hyaloid vasculature morphogenesis in zebrafish: a role for the lens in maturation and maintenance of the hyaloid. Dev. Biol. 394 (2), 327–339.

Hartsock, A., Nelson, W.J., 2008. Adherens and tight junctions: structure, function and connections to the actin cytoskeleton. Biochim. Biophys. Acta 1778 (3), 660–669.

Hero, I., 1989. The optic fissure in the normal and microphthalmic mouse. Exp. Eye Res. 49 (2), 229–239.

Hero, I., 1990. Optic fissure closure in the normal cinnamon mouse. An ultrastructural study. Invest. Ophthalmol. Vis. Sci. 31 (1), 197–216.

Hero, I., Farjah, M., Scholtz, C.L., 1991. The prenatal development of the optic fissure in colobomatous microphthalmia. Invest. Ophthalmol. Vis. Sci. 32 (9), 2622–2635.

Jowett, T., Lettice, L., 1994. Whole-mount in situ hybridizations on zebrafish embryos using a mixture of digoxigenin- and fluorescein-labelled probes. Trends Genet. 10 (3), 73–74.

Kelberman, D., Islam, L., Lakowski, J., Bacchelli, C., Chanudet, E., Lescai, F., Patel, A., Stupka, E., Buck, A., Wolf, S., et al., 2014. Mutation of SALL2 causes recessive ocular coloboma in humans and mice. Hum. Mol. Genet. 23 (10), 2511–2526.

Kim, T.H., Goodman, J., Anderson, K.V., Niswander, L., 2007. Phactr4 regulates neural tube and optic fissure closure by controlling PP1-, Rb-, and E2F1-regulated cell-cycle progression. Dev. Cell 13 (1), 87–102.

Kimmel, C.B., Ballard, W.W., Kimmel, S.R., Ullmann, B., Schilling, T.F., 1995. Stages of embryonic development of the zebrafish. Dev. Dyn.: Off. Publ. Am. Assoc. Anat. 203 (3), 253–310.

Kirby, B.B., Takada, N., Latimer, A.J., Shin, J., Carney, T.J., Kelsh, R.N., Appel, B., 2006. In vivo time-lapse imaging shows dynamic oligodendrocyte progenitor behavior during zebrafish development. Nat. Neurosci. 9 (12), 1506–1511.

Koudijs, M.J., den Broeder, M.J., Groot, E., van Eeden, F.J., 2008. Genetic analysis of

the two zebrafish patched homologues identifies novel roles for the hedgehog signaling pathway. BMC Dev. Biol. 8, 15.
Lalani, S.R., Safiullah, A.M., Fernbach, S.D., Harutyunyan, K.G., Thaller, C., Peterson, L. E., McPherson, J.D., Gibbs, R.A., White, L.D., Hefner, M., et al., 2006. Spectrum of CHD7 mutations in 110 individuals with CHARGE syndrome and genotype-phenotype correlation. Am. J. Hum. Genet. 78 (2), 303–314.
Lawson, N.D., Weinstein, B.M., 2002. In vivo imaging of embryonic vascular development using transgenic zebrafish. Dev. Biol. 248 (2), 307–318.
Lee, J., Willer, J.R., Willer, G.B., Smith, K., Gregg, R.G., Gross, J.M., 2008. Zebrafish blowout provides genetic evidence for Patched1-mediated negative regulation of Hedgehog signaling within the proximal optic vesicle of the vertebrate eye. Dev. Biol. 319 (1), 10–22.
Legate, K.R., Fassler, R., 2009. Mechanisms that regulate adaptor binding to beta-integrin cytoplasmic tails. J. Cell Sci. 122 (Pt 2), 187–198.
Liao, W., Bisgrove, B.W., Sawyer, H., Hug, B., Bell, B., Peters, K., Grunwald, D.J., Stainier, D.Y., 1997. The zebrafish gene cloche acts upstream of a flk-1 homologue to regulate endothelial cell differentiation. Development 124 (2), 381–389.
Liu, C., Widen, S.A., Williamson, K.A., Ratnapriya, R., Gerth-Kahlert, C., Rainger, J., Alur, R.P., Strachan, E., Manjunath, S.H., Balakrishnan, A., et al., 2016. A secreted WNT-ligand-binding domain of FZD5 generated by a frameshift mutation causes autosomal dominant coloboma. Hum. Mol. Genet. 25 (7), 1382–1391.
Liu, Q., Babb, S.G., Novince, Z.M., Doedens, A.L., Marrs, J., Raymond, P.A., 2001. Differential expression of cadherin-2 and cadherin-4 in the developing and adult zebrafish visual system. Vis. Neurosci. 18 (6), 923–933.
Liu, Q., Chen, Y., Pan, J.J., Murakami, T., 2009. Expression of protocadherin-9 and protocadherin-17 in the nervous system of the embryonic zebrafish. Gene Expr. Pattern. 9 (7), 490–496.
Liu, Q., Londraville, R., Marrs, J.A., Wilson, A.L., Mbimba, T., Murakami, T., Kubota, F., Zheng, W., Fatkins, D.G., 2008. Cadherin-6 function in zebrafish retinal development. Dev. Neurobiol. 68 (8), 1107–1122.
Liu, Q., Marrs, J.A., Raymond, P.A., 1999a. Spatial correspondence between R-cadherin expression domains and retinal ganglion cell axons in developing zebrafish. J. Comp. Neurol. 410 (2), 290–302.
Liu, Q., Sanborn, K.L., Cobb, N., Raymond, P.A., Marrs, J.A., 1999b. R-cadherin expression in the developing and adult zebrafish visual system. J. Comp. Neurol. 410 (2), 303–319.
Lupo, G., Gestri, G., O'Brien, M., Denton, R.M., Chandraratna, R.A., Ley, S.V., Harris, W.A., Wilson, S.W., 2011. Retinoic acid receptor signaling regulates choroid fissure closure through independent mechanisms in the ventral optic cup and periocular mesenchyme. Proc. Natl. Acad. Sci. USA 108 (21), 8698–8703.
Macdonald, R., Scholes, J., Strahle, U., Brennan, C., Holder, N., Brand, M., Wilson, S. W., 1997. The Pax protein Noi is required for commissural axon pathway formation in the rostral forebrain. Development 124 (12), 2397–2408.
Masai, I., Lele, Z., Yamaguchi, M., Komori, A., Nakata, A., Nishiwaki, Y., Wada, H., Tanaka, H., Nojima, Y., Hammerschmidt, M., et al., 2003. N-cadherin mediates retinal lamination, maintenance of forebrain compartments and patterning of retinal neurites. Development 130 (11), 2479–2494.
Matsumoto, K., Yoshitomi, H., Rossant, J., Zaret, K.S., 2001. Liver organogenesis promoted by endothelial cells prior to vascular function. Science 294 (5542), 559–563.
Matt, N., Ghyselinck, N.B., Pellerin, I., Dupe, V., 2008. Impairing retinoic acid signalling in the neural crest cells is sufficient to alter entire eye morphogenesis. Dev. Biol. 320 (1), 140–148.
McMahon, C., Gestri, G., Wilson, S.W., Link, B.A., 2009. Lmx1b is essential for survival of periocular mesenchymal cells and influences Fgf-mediated retinal patterning in zebrafish. Dev. Biol. 332 (2), 287–298.
Morris, A.C., 2011. The genetics of ocular disorders: insights from the zebrafish. Birth Defects Res. Part C Embryo Today: Rev. 93 (3), 215–228.
Moser, M., Legate, K.R., Zent, R., Fassler, R., 2009. The tail of integrins, talin, and kindlins. Science 324 (5929), 895–899.
Murphy, D.A., Courtneidge, S.A., 2011. The 'ins' and 'outs' of podosomes and invadopodia: characteristics, formation and function. Nat. Rev. Mol. Cell Biol. 12 (7), 413–426.
Oda, H., Takeichi, M., 2011. Evolution: structural and functional diversity of cadherin at the adherens junction. J. Cell Biol. 193 (7), 1137–1146.
Onwochei, B.C., Simon, J.W., Bateman, J.B., Couture, K.C., Mir, E., 2000. Ocular colobomata. Surv. Ophthalmol. 45 (3), 175–194.
Picker, A., Cavodeassi, F., Machate, A., Bernauer, S., Hans, S., Abe, G., Kawakami, K., Wilson, S.W., Brand, M., 2009. Dynamic coupling of pattern formation and morphogenesis in the developing vertebrate retina. PLoS Biol. 7 (10), e1000214.
Pillai-Kastoori, L., Wen, W., Wilson, S.G., Strachan, E., Lo-Castro, A., Fichera, M., Musumeci, S.A., Lehmann, O.J., Morris, A.C., 2014. Sox11 is required to maintain proper levels of Hedgehog signaling during vertebrate ocular morphogenesis. PLoS Genet. 10 (7), e1004491.
Rainger, J., Pehlivan, D., Johansson, S., Bengani, H., Sanchez-Pulido, L., Williamson, K.A., Ture, M., Barker, H., Rosendahl, K., Spranger, J., et al., 2014. Monoallelic and biallelic mutations in MAB21L2 cause a spectrum of major eye malformations. Am. J. Hum. Genet. 94 (6), 915–923.
Rainger, J., van Beusekom, E., Ramsay, J.K., McKie, L., Al-Gazali, L., Pallotta, R., Saponari, A., Branney, P., Fisher, M., Morrison, H., et al., 2011. Loss of the BMP antagonist, SMOC-1, causes Ophthalmo-acromelic (Waardenburg Anophthalmia) syndrome in humans and mice. PLoS Genet. 7 (7), e1002114.
Saint-Geniez, M., D'Amore, P.A., 2004. Development and pathology of the hyaloid, choroidal and retinal vasculature. Int. J. Dev. Biol. 48 (8–9), 1045–1058.
Sakaguchi, T.F., Sadler, K.C., Crosnier, C., Stainier, D.Y., 2008. Endothelial signals modulate hepatocyte apicobasal polarization in zebrafish. Curr. Biol. 18 (20), 1565–1571.
Sanyanusin, P., Schimmenti, L.A., McNoe, L.A., Ward, T.A., Pierpont, M.E., Sullivan, M. J., Dobyns, W.B., Eccles, M.R., 1995. Mutation of the PAX2 gene in a family with optic nerve colobomas, renal anomalies and vesicoureteral reflux. Nat. Genet. 9 (4), 358–364.
Schimmenti, L.A., de la Cruz, J., Lewis, R.A., Karkera, J.D., Manligas, G.S., Roessler, E., Muenke, M., 2003. Novel mutation in sonic hedgehog in non-syndromic colobomatous microphthalmia. Am. J. Med. Genet. Part A 116A (3), 215–221.
Schmitt, E.A., Dowling, J.E., 1994. Early eye morphogenesis in the zebrafish, BrachyDanio rerio. J. Comp. Neurol. 344 (4), 532–542.
Scholtz, C.L., Chan, K.K., 1987. Complicated colobomatous microphthalmia in the microphthalmic (mi/mi) mouse. Development 99 (4), 501–508.
See, A.W., Clagett-Dame, M., 2009. The temporal requirement for vitamin A in the developing eye: mechanism of action in optic fissure closure and new roles for the vitamin in regulating cell proliferation and adhesion in the embryonic retina. Dev. Biol. 325 (1), 94–105.
Stainier, D.Y., Weinstein, B.M., Detrich 3rd, H.W., Zon, L.I., Fishman, M.C., 1995. Cloche, an early acting zebrafish gene, is required by both the endothelial and hematopoietic lineages. Development 121 (10), 3141–3150.
Take-uchi, M., Clarke, J.D., Wilson, S.W., 2003. Hedgehog signalling maintains the optic stalk-retinal interface through the regulation of Vax gene activity. Development 130 (5), 955–968.
Torres, M., Gomez-Pardo, E., Gruss, P., 1996. Pax2 contributes to inner ear patterning and optic nerve trajectory. Development 122 (11), 3381–3391.
Tsuji, N., Kita, K., Ozaki, K., Narama, I., Matsuura, T., 2012. Organogenesis of mild ocular coloboma in FLS mice: failure of basement membrane disintegration at optic fissure margins. Exp. Eye Res. 94 (1), 174–178.
Uribe, R.A., Gross, J.M., 2007. Immunohistochemistry on cryosections from embryonic and adult zebrafish eyes. CSH Protoc., 779.
van den Dries, K., Bolomini-Vittori, M., Cambi, A., 2014. Spatiotemporal organization and mechanosensory function of podosomes. Cell Adhes. Migr. 8 (3), 268–272.
Wada, N., Javidan, Y., Nelson, S., Carney, T.J., Kelsh, R.N., Schilling, T.F., 2005. Hedgehog signaling is required for cranial neural crest morphogenesis and chondrogenesis at the midline in the zebrafish skull. Development 132 (17), 3977–3988.
Wang, Y., Kaiser, M.S., Larson, J.D., Nasevicius, A., Clark, K.J., Wadman, S.A., Roberg-Perez, S.E., Ekker, S.C., Hackett, P.B., McGrail, M., et al., 2010. Moesin1 and Ve-cadherin are required in endothelial cells during in vivo tubulogenesis. Development 137 (18), 3119–3128.
Westenskow, P., Piccolo, S., Fuhrmann, S., 2009. Beta-catenin controls differentiation of the retinal pigment epithelium in the mouse optic cup by regulating Mitf and Otx2 expression. Development 136 (15), 2505–2510.
Westerfield, M., 1995. The Zebrafish Book: A Guide for the Laboratory use of Zebrafish (Danio rerio). University of Oregon, Eugene, OR.
Weston, C.R., Wong, A., Hall, J.P., Goad, M.E., Flavell, R.A., Davis, R.J., 2003. JNK initiates a cytokine cascade that causes Pax2 expression and closure of the optic fissure. Genes Dev. 17 (10), 1271–1280.
Williams, A.L., Bohnsack, B.L., 2015. Neural crest derivatives in ocular development: discerning the eye of the storm. Birth Defects Res. Part C Embryo Today: Rev. 105 (2), 87–95.
Williamson, K.A., Rainger, J., Floyd, J.A., Ansari, M., Meynert, A., Aldridge, K.V., Rainger, J.K., Anderson, C.A., Moore, A.T., Hurles, M.E., et al., 2014. Heterozygous loss-of-function mutations in YAP1 cause both isolated and syndromic optic fissure closure defects. Am. J. Hum. Genet. 94 (2), 295–302.
Wu, S.K., Gomez, G.A., Michael, M., Verma, S., Cox, H.L., Lefevre, J.G., Parton, R.G., Hamilton, N.A., Neufeld, Z., Yap, A.S., 2014. Cortical F-actin stabilization generates apical-lateral patterns of junctional contractility that integrate cells into epithelia. Nat. Cell Biol. 16 (2), 167–178.
Ye, M., Berry-Wynne, K.M., Asai-Coakwell, M., Sundaresan, P., Footz, T., French, C.R., Abitbol, M., Fleisch, V.C., Corbett, N., Allison, W.T., et al., 2010. Mutation of the bone morphogenetic protein GDF3 causes ocular and skeletal anomalies. Hum. Mol. Genet. 19 (2), 287–298.

Please cite this article as: James, A., et al., (2016), http://dx.doi.org/10.1016/j.ydbio.2016.09.008